Techno-economic assessment of chemical looping reforming of Natural Gas for Hydrogen production and power generation with integrated CO_2 capture

Shareq Mohd Nazir[1], Joana Francisco Morgado[1,2], Olav Bolland[1], Rosa Quinta-Ferreira[2], Shahriar Amini[1,3*]

[1]Department of Energy and Process Engineering, Norwegian University of Science and Technology, Trondheim, Norway
[2]Department of Chemical Engineering, University of Coimbra, Coimbra, Portugal
[3]SINTEF Industry, Trondheim, Norway

Abstract:

The current study presents the techno-economic analysis of the CLR-CC process. The CLR-CC process comprises of chemical looping reforming (CLR) of Natural Gas, water gas shift, CO_2 capture and compression, and combined cycle power plant. A 1-D phenomenological model was developed using MATLAB and is used to study the performance of CLR, whereas the remaining part of the process was analysed using commercial software tools like Aspen and Thermoflow. The effect of design conditions in CLR, mainly the air flowrate to the oxidation reactor, oxidation reactor outlet temperature and the steam flowrate to the fuel reactor of CLR, on the overall techno-economic performance of the CLR-CC process is reported. The CH_4 conversion in CLR, net electrical efficiency, CO_2 avoidance rate and the Levelised Cost of Electricity (LCOE) have been identified as techno-economic performance indicators. For the sensitivity study carried out in this study through 12 cases, the net electrical efficiency of the CLR-CC process varies between 40.0 and 43.4 %, whereas the LCOE varies between 75.3 and 144.8 $/MWh, which is highly dependent on the fuel cost and process contingency rates.

*Corresponding author
Email: shahriar.amini@sintef.no
Telephone: +47- 46639721
Address: S. P. Andersens veg 15 B, Trondheim, 7031

Keywords: Pre-combustion CO_2 capture method; Chemical Looping Reforming; Combined cycle power plants; Techno-economic analysis.

Nomenclature:

BEC	Bare Erected Cost
CCS	Carbon Capture and Sequestration
CLC	Chemical Looping Combustion
CLR	Chemical Looping Reforming
CF	Capacity Factor
EPCC	Engineering Procurement and Construction Cost
FC	Fuel Cost
FCF	Fixed Charge Factor
FOM	Fixed Operating and Maintenance
GT	Gas Turbine
HP	High Pressure
HR	Heat Rate
HRSG	Heat Recovery Steam Generator
HTS	High Temperature Shift
LCOE	Levelised Cost of Electricity
LP	Low Pressure
LTS	Low Temperature Shift
MP	Medium Pressure
NG	Natural Gas
ST	Steam Turbine
TCR	Total Capital Requirement
TOC	Total Overnight Cost
TPC	Total Plant Cost
VOM	Variable Operating and Maintenance
WGS	Water Gas Shift
η	Net Electrical Efficiency

1. Introduction

While the energy transition is taking momentum and a shift towards renewables is evidently visible, oil, coal and natural gas still account for more than 80% of the world's primary energy demand (WEO 2016). There needs to be strike between satisfying the energy demands and the control of CO_2 levels in the atmosphere, as CO_2 is the major contributor to the greenhouse gas emissions. Carbon Capture and Sequestration (CCS) is one of the methods to mitigate greenhouse gas emissions and is foreseen to reduce one sixth of the total CO_2 emissions by 2050 (ETP 2012). Three main CO_2 capture routes have been studied and presented in literature, which are pre-, post- and oxy-combustion. A detailed review on the developments in the capture methods have been presented by Boot-Handford et al. (2014). The focus of this paper is on a pre-combustion capture method in Natural Gas (NG) based power plants with Chemical Looping Reforming (CLR).

Chemical Looping (CL) processes with their ability to inherently separate air and CO_2 have attracted a lot of research attention. CL processes like Chemical Looping Combustion (CLC)

and Chemical Looping Reforming (CLR) use metallic oxygen carriers to convert the chemical potential of fossil fuels into work. The concept of chemical looping was first proposed by Richter and Knoche (1983) and was applied to study the CLC based power plant by Ishida, Zheng, and Akehata (1987), Ishida and Jin (1994). CLC completely converts the chemical exergy of fuel into heat at low temperatures (Iloeje, Zhao, and Ghoniem 2015, Naqvi and Bolland 2007, Consonni et al. 2006) whereas CLR converts the chemical exergy of fossil fuel into chemical exergy of hydrogen rich fuel (Nazir, Bolland, and Amini 2017, de Diego et al. 2009, Rydén, Lyngfelt, and Mattisson 2006).

Figure 1 shows the schematic of a CLR process, which comprises of oxidation reactor and fuel reactor. Compressed air oxidizes the metallic oxygen carrier in the oxidation reactor and produces metal oxide and a depleted air stream (N_2-rich stream). The metal oxide then reacts with NG in the fuel reactor in presence of steam to produce syngas and regenerate the metallic oxygen carrier, which is re-circulated to the oxidation reactor. The current state-of-the-art for CLR is given in a number of studies; on choice of oxygen carrier (Tang, Xu, and Fan 2015, Adanez et al. 2012), reactor scale modeling and experimental studies (Spallina, Gallucci, et al. 2016, Francisco Morgado et al. 2016, Diglio et al. 2016, Yahom et al. 2014, Bischi et al. 2012, Pröll et al. 2011, Pröll et al. 2010, de Diego et al. 2009, Rydén, Lyngfelt, and Mattisson 2006). Studies have also been reported on hydrogen production for power generation by Ca-Cu looping processes (Abanades et al. 2010, Martínez et al. 2014), auto-thermal reforming (Romano, Chiesa, and Lozza 2010, Nord, Anantharaman, and Bolland 2009, Corradetti and Desideri 2005, Lozza and Chiesa 2000a, Zohrabian et al. 2016, Ding and Chan 2008, Fiaschi et al. 2005) and steam-methane reforming (Lozza and Chiesa 2000b, Antzara et al. 2015).

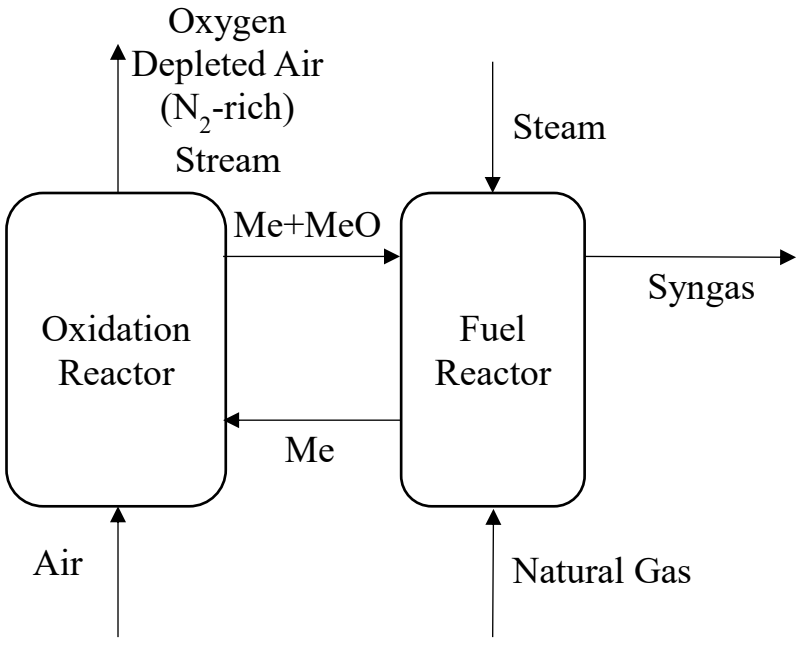

Figure 1: Schematic of a CLR process

Analysis of power plants with pre-combustion capture in NG based plants have been presented by Fan and Zhu (2015), Cormos, Petrescu, and Cormos (2014), Martínez et al. (2013), Cormos (2012), Kvamsdal, Jordal, and Bolland (2007). Techno-economic analysis of combined cycle with CO_2 capture have been studied by Mathieu and Bolland (2013), Zohrabian et al. (2016),

Spallina, Pandolfo, et al. (2016), Mantripragada and Rubin (2013). The cited literature focuses on pre-combustion methods with hydrogen production through different routes like Ca-Cu looping, steam-methane reforming, auto-thermal reforming and membrane assisted reforming. Anyhow, this paper focuses on the techno-economic analysis of CLR-CC process using the 1-D generic phenomenological model for fluidized bed CLR (Francisco Morgado et al. 2016). The CLR-CC process has been defined by Nazir, Bolland, and Amini (2017). The CLR-CC process combines the reforming of NG in CLR, followed by Water Gas Shift (WGS) process, CO_2 capture and compression to produce a H_2-rich stream, which is used in a combined cycle power plant to produce electricity. The technical performance of the CLR-CC process is studied at different design conditions in the CLR. Net electrical efficiency and CO_2 avoidance rates have been chosen as indicators of technical performance. The effect of air flowrate and temperature at the outlet of oxidation reactor and the steam flow rate in fuel reactor of CLR on the techno-economic behavior of the CLR-CC process is shown in this study. The Levelised Cost of Electricity (LCOE) and cost of CO_2 avoidance is estimated for the CLR-CC process. Based on the results, the effect of fuel costs and process contingencies on the LCOE is also presented in this study. The remainder of the sections have the description of the process, the methodology, results and discussions followed by conclusions.

2. Process Description

Figure 2 shows the schematic of the CLR-CC process. The choice of the design pressure for the CLR and the selection of process systems for the CLR-CC process have been discussed and presented by Nazir, Bolland, and Amini (2018). The design pressure for the CLR is 18 bar. Compressed air at 18 bar reacts with the metallic oxygen carrier in the oxidation reactor. The compressed air is a mixture of air bled from the GT system and the atmospheric air, which is compressed in an additional air compressor. The amount of air bled from the GT system is equal to 12% of the total airflow in the GT. The overall energy penalty is less when the air bled from the GT system is used. Anyhow extracting too much air from the GT system before the combustion chamber might affect the performance and temperature profiles of the GT (Nord, Anantharaman, and Bolland 2009). The metal-metal oxide considered in the current study is Ni-NiO system. A mixture of Ni-NiO leaves the oxidation reactor along with the air stream, which is depleted in Oxygen (N_2-rich stream). The NiO from the mixture then reacts with NG (100% CH_4 in this study) in the presence of steam in the fuel reactor of CLR. The methane is reformed to syngas and NiO is reduced to Ni. The overall reactions taking place in the CLR unit (reactions 1 and 2) are shown below.

$$0.5\,O_2 + Ni \leftrightarrow NiO \qquad (1)$$

$$CH_4 + NiO \leftrightarrow CO + 2\,H_2 + Ni \qquad (2)$$

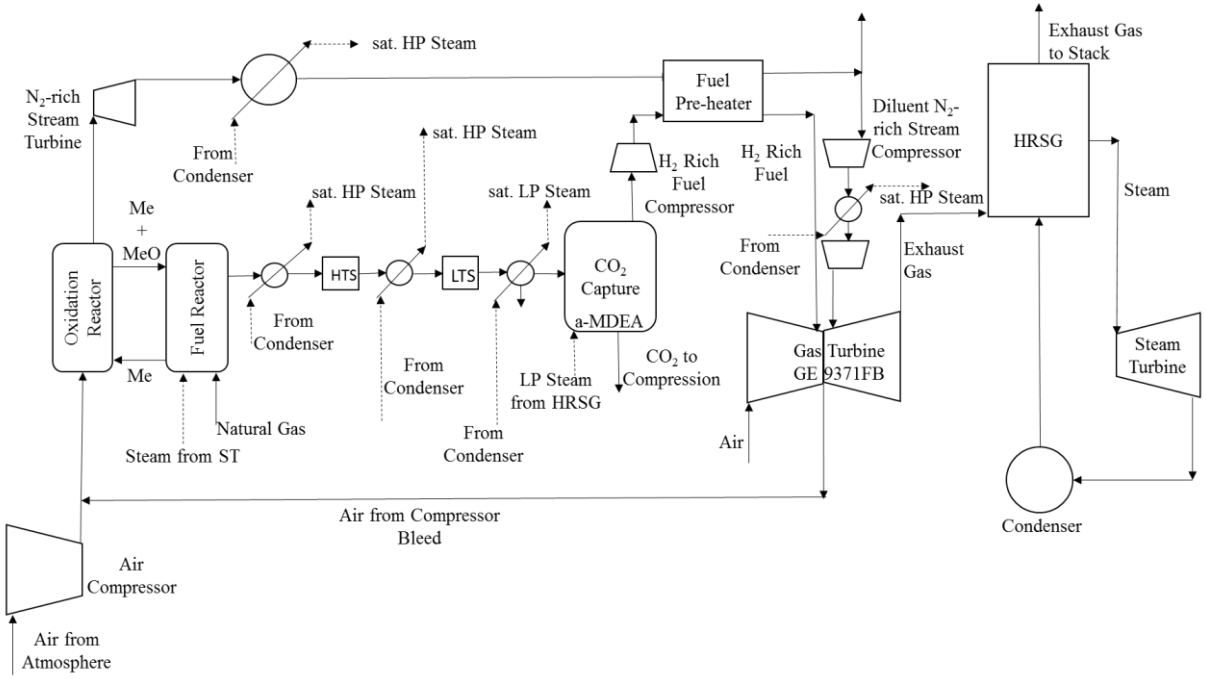

Figure 2: Schematic of the CLR-CC process

The syngas from the fuel reactor is cooled down and sent through high (HTS) and low temperature (LTS) WGS reactors where most of the CO and H_2O is converted to CO_2 and H_2. Syngas and the HTS product stream are cooled down to produce saturated High Pressure (HP) steam at 174.4 bar. The pressure at which steam is produced is dependent on the point it is being integrated within the steam cycle. The product stream from LTS is cooled down to 50 °C. Saturated Low Pressure (LP) steam at 3.8 bar is produced from cooling of LTS product. The final gaseous mixture contains mainly CO_2 and H_2 and is ready for CO_2 capture. CO_2 is absorbed in the absorber using the a-MDEA amine and H_2-rich fuel is collected at the top. The rich amine solution is then flashed and pre-heated before entering the regenerator. The amine is regenerated and is sent to the absorber, whereas the CO_2 stream is compressed and prepared for storage.

The H_2-rich fuel from the top of the absorber is compressed, preheated and sent to the Gas Turbine (GT) for combustion with air. 12% of the compressed air in the GT, about 277 TPH from each GT system, is extracted as bleed from the compressor discharge and is used in the oxidation reactor of CLR. The N_2-rich stream from the oxidation reactor is expanded in a turbine to extract work and then is cooled down by producing saturated HP steam at 174.4 bar and pre-heating the H_2-rich fuel. Fraction of the N_2-rich stream, equal to the mass of air bled from the GT, is compressed and used as a diluent in the GT. The inter-stage cooling during compression of N_2-rich stream is also used to produce saturated HP steam at 174.4 bar. Similar approach to treat the N_2-rich stream has been followed in Nazir, Bolland, and Amini (2018). Several other process alternatives were considered by the authors to treat the N_2-rich stream. For example, cooling the fraction of N_2-rich stream from the oxidation reactor, which is used as a diluent in the GT system, and compressing it to the desired pressure in the GT. Anyhow, the authors noticed that treating the N_2-rich stream as presented in this study has less efficiency penalty on the overall process.

The power plant is a combined cycle with two gas turbines, two Heat Recovery Steam Generators (HRSG) and one steam turbine (ST) system, as it is the same configuration used for a NGCC plant without capture in EBTF (2011). The steam cycle is a three-pressure level with reheat and comprises of one high pressure steam turbine, one medium pressure steam turbine and two flow low pressure turbines. The low pressure (LP), medium pressure (MP) and high pressure (HP) steam levels are maintained at 3.4, 32.7 and 166 bar, respectively. The water and steam mixture from the ST is condensed in a water-cooled condenser before the water is pumped and sent to HRSG. The cooling water requirements in the process is met by a natural draft cooling tower. The saturated HP and LP steam generated from cooling of process streams in the process is added to the HRSG at the inlet of respective HP and LP superheaters. The assumptions made in the model are explained in the following section.

3. Methodology

The techno-economic assessment of the CLR-CC process was carried out using the process models to assess different sections of the process, and the economic model as described by GCCSI (2013). The description of the models and the respective assumptions alongside criteria for technical assessment is briefed below.

3.1. 1-D Model for CLR

The 1-D model used in this work consists of a 1-D generic phenomenological model for fluidized bed reactors applied to CLR (Morgado et al. 2016) developed using MATLAB. The generic model formulation is based on the averaging probabilistic approach developed by Thompson et al. (Thompson, Bi, and Grace 1999, Abba et al. 2003) and couples the three most frequent fluidization regimes in industry (bubbling, turbulent and fast fluidization). Furthermore, it relies on the two-phase theory that distinguishes between a low and high dense phase, poor and highly concentrated in solids, respectively. The material and energy balances as well as the empirical closure laws used to describe the hydrodynamics of the system under different fluidization regimes are described by Morgado et al. (2016). The use of kinetic models like this one helps in evaluating the process more accurately at different design conditions and dynamics of the process. In this work the Dual Circulating Fluidized Bed (DCFB) configuration proposed by (Pröll et al.) was considered. Therefore, both reactors operate under the same fluidization regimes that is turbulent and/or fast fluidization (Schmid et al. 2011, Kolbitsch et al. 2009).

Adiabatic conditions were assumed in both oxidation and fuel reactors. The temperature at the outlet of the oxidation reactor was limited to 1200 ± 10 °C due to the thermal degradation of the oxygen carrier and was used to estimate the oxygen carrier circulation rate between the oxidation and fuel reactors. In addition, the effect of changing the temperature at the outlet of oxidation reactor to 1100 ± 10 °C is also presented in this paper. The air flowrate entering the oxidation reactor was defined to meet higher conversion rates of methane in the fuel reactor. The amount of steam flowrate fed to the fuel reactor was assumed based on the CO/H_2O ratio required for favorable conditions in WGS.

The dimensions of the reactors (height and diameter) were established in order to meet the equilibrium conversions in the fuel reactor alongside maintaining the fluidization regimes as in DCFB. Due to the excellent heat transfer properties of fluidized bed reactors, the temperature

in the low and high dense phases was considered equal. The superficial velocity of the gas inside the reactors has been constrained so that it is always higher or equal to the minimum fluidization velocity. The particle size of the oxygen carrier is assumed 250 μm.

3.2. WGS and CO_2 capture model

The WGS reactors, CO_2 capture and compression processes were simulated in ASPEN Hysys V8.6 (AspenHYSYS 2017). Peng-Robinson thermodynamic model is considered for the WGS and CO_2 compression sections, whereas Acid-Gas Model is used to estimate the equilibrium conditions in CO_2 capture section. The HTS and LTS are modeled using steady state equilibrium reactor modules with adiabatic conditions. The inlet streams to the HTS and LTS reactors are at 400 °C and 200 °C respectively. The pressure drop in the WGS reactors is assumed 3%. The pressure drop considered in the heat exchangers in the entire process is 2% for gaseous streams and 0.4 bar for liquid streams (EBTF 2011).

The main design conditions in the CO_2 capture section are listed in Table 1. The amine used to absorb CO_2 is a-MDEA (45% by mass in the solution), which is used for moderate partial pressures of CO_2 (3-4 bar) at the absorber inlet (Nord, Anantharaman, and Bolland 2009) and 5% by mass Piperazine is used as an activator. The capture rate of 95% is assumed across the absorber and the flowrate of amine is estimated. Superheated LP steam extracted from the inlet of the LP steam turbine at 3.4 bar and 270 °C is used in the reboiler of the regenerator. CO_2 captured is compressed and pumped to 110 bar in three compression stages followed by pumping as described in EBTF (2011).

Number of absorber trays	20
Number of stripper trays	20
Pressure drop in the absorber (bar)	0.1
Pressure drop in the regenerator (bar)	0.1
Lean amine loading (mol CO_2/mol MDEA)	0.301
MDEA/water (mass/mass)	1
Condenser Temperature in regenerator (°C)	46.11
Adiabatic efficiency of pump for regenerated amine (%)	80

Table 1: Design conditions in CO_2 capture section (Nazir, Bolland, and Amini 2017)

3.3. Power Plant

The combined cycle power plant has been analysed using Thermoflex component of the Thermoflow Suite (Thermoflow 2017). The GT system chosen for the analysis is GE-9371FB, which is robust to changes in fuel composition and is favorable for H_2-rich fuels (EBTF 2011, Nord, Anantharaman, and Bolland 2009). The power plant comprises of two GTs, two HRSGs and one ST system. The ST system is a three steam level with reheat. The steam levels are 3.4/32.7/166 bar. The GT is run at full load conditions for all the cases considered in this paper and hence the fuel input to the GT is estimated accordingly. 12% of the compressed air is bled at the compressor discharge in the GT and used in the CLR oxidation reactor. The N_2-rich stream from the fuel reactor of CLR is added in the combustor along with the fuel not only to compensate for the mass of air bled from the GT system, but also to act as a diluent which reduces the flame temperature when H_2-rich fuel is combusted (Chiesa, Lozza, and Mazzocchi 2005).

228 3.4. Economic Model

229 The LCOE and the cost of CO_2 avoidance are the main performance indicators for the economic
230 analysis of the process. The economic analysis to assess the LCOE and cost of CO_2 avoidance
231 for the process is carried out using the methodology proposed by the GCCSI (2013). The LCOE
232 for the CLR-CC process is estimated using the following equation 1:

233 $$LCOE = \frac{(TCR)(FCF)+FOM}{(MW)(CF\times 8766)} + VOM + (HR)(FC) \qquad \text{Equation (1)}$$

234 The nomenclature used in equation 1 is given in Table 2.

Parameter	Definition	Unit
TCR	Total Capital Requirement in the base year of the analysis	$
FCF	Fixed Charge Factor as defined in equation 2	fraction
FOM	Fixed O&M costs	$/year
MW	Net power output of the plant	MW
CF	Capacity Factor – availability of the plant	Fraction
VOM	Variable O&M costs excluding the fuel costs	$/MWh
HR	Net power plant heat rate	MJ/MWh
FC	Fuel Cost per unit of energy	$/MJ

235 *Table 2: Nomenclature for parameters used to estimate LCOE in equation 1*

236 The FCF is calculated using equation (2) where "*r*" is the interest rate or discount rate and *T* is
237 the economic life of the plant relative to the base year of analysis used in the study. Furthermore,
238 an interest rate of 10% and an economic life of the plant of 30 years were assumed.

239 $$FCF = \frac{r(1+r)^T}{(1+r)^T-1} \qquad \text{Equation (2)}$$

240 The TCR is estimated using the methodology as shown in Table 3.

Component	Definition
Bare Erected Cost (BEC)	Sum of installed cost of equipment
Engineering Procurement Construction Costs (EPCC)	10% of BEC
Process Contingency	40%+ of BEC
Project Contingency	15 - 30 % of (BEC +EPCC + Process Contingency)
Total Contingencies	Process Contingency + Project Contingency
Total Plant Costs (TPC)	BEC +EPCC + Total Contingencies
Owners Cost	20.2% of TPC (NETL 2011)
Total Overnight Costs (TOC)	TPC + Owners Cost
Total Capital Requirement (TCR)	1.14*TOC (NETL 2011)

241 *Table 3: Methodology to estimate TCR*

242 The Sizing and Economics tool in ASPEN Hysys V8.6 and the PEACE component in
243 Thermoflow V26 is used to estimate the installation costs of the process equipment except the
244 oxidation and fuel reactors of CLR. The LCOE for the NGCC without capture case estimated
245 using the BEC from the database of commercial software tools, like Aspen Hysys and
246 Thermoflow, is validated against the LCOE reported in the DOE/NETL (2007) considering

similar fuel costs. The costs of the basic equipment considered in this paper are from the reference year 2016, and hence, correction factors have not been introduced. The BEC of high temperature and high pressure reactors is difficult to estimate and the cost data is not readily available. Hence, the methodology described in Peters and Timmerhaus (1991) is used to estimate the cost of the oxidation and fuel reactors of CLR, where the weight of the reactor is calculated first. The height and diameter of the oxidation and fuel reactors were considered 6 m and 6 m, respectively since the equilibrium conditions are reached within those dimensions. The weight of each reactor is calculated to be 364750 lb. A reference cost of the reactor similar to that of Fluidized Catalytic Cracker is used in this study (Spallina, Pandolfo, et al. 2016). The reference cost assumed is 8.2 M$ for 130000 lb. With a scale factor of 0.6, the cost of each reactor is 15.23 M$. Considering installation cost to be 80% of the cost of the reactor, the BEC for each reactor is 27.4 M$. The transport disengaging height (TDH) in the reactor is not considered in this study, since the height of the reactor assumed is enough to reach equilibrium conditions. Considering TDH, i.e. assuming 20 m height of the reactor instead of 6 m in this study will increase the BEC of the CLR by 30% but has less than 1% effect on the LCOE of the process.

As seen in Table 3, the process contingency is 40%+ of the BEC as the process is a new concept with limited data. However, in this study, the process contingency is assumed 50% of BEC for the CLR-CC process. On the other hand, a NGCC plant without capture will have a process contingency of 10% of BEC, as it is already a commercially available technology. A project contingency of 30% of sum of BEC, EPCC and process contingency is assumed in this study for all the cases. The TCR/TOC ratio of 1.14 is assumed for the CLR-CC process as the project is assumed a high-risk investor owned utility (NETL 2011).

The assumptions made to estimate the operating and maintenance (O&M) costs is shown in Table 4.

Fixed O&M Costs		
Operating Labor	1.7	M$
Maintenance, Support and Administrative Labor	2.5	% of TOC
Property Taxes	Included in insurance costs	
Insurance costs	2	% of TOC
Cost of NG (Fuel Cost)	10.18	$/GJ LHV
Variable O&M Costs		
Consumables		
Cooling Water Make Up Costs	0.39	$/m3
Process Water Cost	2.22	$/m3
Catalysts and Sorbent Replacement		
Oxygen Carrier cost	15	$/kg
WGS catalyst cost	15574	$/m3
Amine cost	2298.3	$/m3
Replacement Period	5	Years
CO_2 Transport and Storage Costs	11.12	$/ton CO_2
Emissions Tax (CO_2 tax)	27.22	$/ton CO_2

Table 4: Assumptions to calculate O&M costs

After estimating the LCOE of the CLR-CC process, the cost of CO_2 avoided is estimated by equation (3).

$$Cost\ of\ CO_2\ avoided\ \left(\frac{\$}{tCO_2}\right) = \frac{LCOE_{CLR\_CC} - LCOE_{NGCC}}{\left(\frac{tCO_2}{MWh}\right)_{NGCC} - \left(\frac{tCO_2}{MWh}\right)_{CLR\_CC}} \quad \text{Equation (3)}$$

3.5. Criteria for techno-economic assessment

The performance of CLR affects the overall performance of the CLR-CC process. The conditions of pressure, temperature and compositions of the product streams from the CLR affect the fuel flowrates in the process, the turbines and compressor work, and amount of steam produced from the cooling of high temperature process streams. The available manipulative variables in the process are the air flowrate (O_2 flowrate) to the oxidation reactor, the outlet temperature of the oxidation reactor, the amount of steam added in the fuel reactor and the design pressure in the oxidation reactor. The impact of pressure inside the oxidation reactor is not included in this work and it forms a part of another article. Thus, only the remaining three independent variables (air flowrate, oxidation reactor outlet temperature and amount of steam to the fuel reactor) were studied in this work. To evaluate the performance of the CLR-CC process while manipulating these independent variables, different performance indicators were defined. The conversion of CH_4 and the oxygen carrier utilization are the main performance indicators for the CLR process. The CO_2 avoidance and the net electrical efficiency are the performance indicators considered for the CLR-CC process. The LCOE is the main performance indicator for the economic performance of the process. The CO_2 avoidance and net electrical efficiency are defined as follows:

$$CO_2\ Avoidance\ (\%) = \frac{100 \times (CO_2\ emitted\ in\ NGCC\ without\ capture - CO_2\ emitted\ in\ NGCC\ with\ capture)}{CO_2\ emitted\ in\ NGCC\ without\ capture} \quad \text{Equation (4)}$$

$$Net\ Electrical\ Efficiency\ (\eta) = \frac{100 \times Net\ electricity\ produced\ from\ the\ overall\ process}{LHV\ of\ NG\ input\ to\ the\ process} \quad \text{Equation (5)}$$

Considering the amount of air flowrate to the oxidation reactor, the stoichiometry given by the reforming reaction of CH_4 implies that 0.5 moles of O_2 are needed to reform CH_4 into CO and H_2 (Reaction 3).

$$CH_4 + 0.5\ O_2 \rightarrow CO + 2\ H_2 \qquad (3)$$

Hence, the availability of oxygen in the fuel reactor through the metal oxide (NiO) plays an important role in the conversion of CH_4. A sensitivity study was carried out varying the amount of oxygen entering the CLR by considering the stoichiometric molar ratio of O_2/CH_4 in the system to be 0.5, 0.75 and 0.9. In these cases, the temperature at the outlet of oxidation reactor was assumed to be 1200 ± 10 °C and the steam/CH_4 ratio by mass was assumed to be 1. The equilibrium conversion of CH_4 at different O_2/CH_4 molar ratio is shown in Table 5.

O_2:CH_4 (mol/mol)	Conversion of methane (%)
0.5	50.6
0.75	81.9
0.9	96.2

Table 5: Sensitivity study to decide the O_2/CH_4 ratio

As seen in Table 5, the conversion of CH_4 increases with an increase in O_2/CH_4 ratio at the inlet of the CLR. Hence, further sensitivity studies in this paper have been reported with an O_2/CH_4 molar ratio of 0.8 and 0.9, where the conversion of CH_4 in the fuel reactor is more than 90%. The overall techno-economic performance of the system was assessed for O_2/CH_4 ratios of 0.8 and 0.9, steam/CH_4 ratio by mass of 0.5, 1 and 1.5 and using oxidation reactor outlet temperatures equal to 1200 °C and 1100 °C. The different cases studied within this work are defined in Table 6. The N_2-rich stream temperature at the inlet of the N_2-rich stream turbine is same as the oxidation reactor outlet temperature. Although the temperature at the inlet of the N_2-rich stream turbine is very high in this analysis where the focus is on identifying the potential of the process, it should be noted that in real case scenario, the temperatures are limited by the maximum allowable temperature suitable for the rotor blades in the turbine. The amount of CH_4 flow to the fuel reactor is based on matching the amount of H_2-rich fuel required to maintain a constant 1.55 GW LHV at the inlet of GT system. Any excess H_2-rich stream produced from the reforming process is also reported.

Cases	O_2/CH_4 by moles	Steam/CH_4 by mass	Oxidation Reactor Outlet Temperature (°C)	CH_4 flow (TPH)
1	0.9	0.5	1200	170
2	0.9	1	1200	170
3	0.9	1.5	1200	172
4	0.9	0.5	1100	170
5	0.9	1	1100	170
6	0.9	1.5	1100	170
7	0.8	0.5	1200	160
8	0.8	1	1200	160
9	0.8	1.5	1200	160
10	0.8	0.5	1100	160
11	0.8	1	1100	160
12	0.8	1.5	1100	160

Table 6: Definition of cases for techno-economic analysis

4. Results and discussion

The main results of the techno-economic analysis of the CLR-CC process for the cases defined in Table 6 are shown in Table 7 and Table 8. Table 7 presents the conditions and results in the CLR at different design conditions with respect to air flowrate (O_2/CH_4 mole ratio), oxidation reactor outlet temperature and steam flowrate in the fuel reactor. Table 8 presents the results for the overall process behavior. The '+' and '-' signs in Table 8 indicates whether the components in the process add or negate the net electrical efficiency respectively. The discussion on these results is presented in this section.

Cases		1	2	3	4	5	6	7	8	9	10	11	12
Oxidation reactor													
Outlet temperature	°C	1200	1200	1200	1105	1100	1100	1200	1200	1200	1100	1100	1100
Outlet pressure	bar	17.94	17.96	17.94	17.93	17.93	17.93	17.80	17.81	17.81	17.74	17.74	17.75
Oxygen carrier flowrate	TPH	12289	9291	7925	22660	18612	13367	6968	6096	5566	11860	9443	8189
N_2-rich stream flowrate	TPH	1005	1006	1017	1005	1005	1005	841	841	841	841	841	841
Fuel Reactor													
Outlet temperature	°C	973	902	843	977	943	882	864	816	778	894	841	801
Outlet pressure	bar	17.50	17.87	17.68	17.50	17.59	17.69	17.43	17.46	17.51	17.45	17.48	17.54
Syngas flowrate	TPH	560	644	739	560	645	730	495	575	655	495	575	655
Methane conversion	%	98.9	96.6	95.3	98.9	98.8	97.5	91.0	88.3	85.9	94.0	91.5	89.2

338 *Table 7: Design conditions and results from CLR*

Cases	Units	1	2	3	4	5	6	7	8	9	10	11	12
Gas Turbine	%-LHV	+25.8	+25.8	+25.4	+25.8	+25.8	+25.8	+27.2	+27.2	+27.2	+27.3	+27.3	+27.3
Steam Turbine	%-LHV	+18.4	+17.4	+16.4	+18.4	+17.8	+17.0	+18.6	+17.6	+16.9	+18.6	+17.8	+17.1
N_2-rich Stream Turbine	%-LHV	+9.6	+9.6	+9.7	+9.0	+9.0	+9.0	+8.5	+8.5	+8.5	+8.0	+8.0	+8.0
Diluent N_2 Stream Compressor	%-LHV	-4.1	-4.1	-4.1	-4.2	-4.2	-4.2	-4.4	-4.4	-4.4	-4.4	-4.4	-4.4
H_2 rich fuel Compressor	%-LHV	-0.8	-0.7	-0.7	-0.7	-0.8	-0.8	-0.8	-0.7	-0.7	-0.8	-0.8	-0.8
Air Compressor	%-LHV	-3.8	-3.8	-3.8	-3.8	-3.8	-3.8	-2.9	-2.9	-2.9	-2.9	-2.9	-2.9
Pump for Regenerated Amine	%-LHV	-0.1	-0.1	-0.1	-0.1	-0.1	-0.1	-0.1	-0.1	-0.1	-0.1	-0.1	-0.1
CO_2 Compressors and Pump	%-LHV	-1.7	-1.8	-1.8	-1.7	-1.8	-1.8	-1.6	-1.6	-1.6	-1.6	-1.7	-1.7
Auxiliaries	%-LHV	-1.1	-1.1	-1.0	-1.1	-1.1	-1.1	-1.1	-1.1	-1.1	-1.1	-1.1	-1.1
Net LHV Input	MW	2363	2363	2391	2363	2363	2363	2224	2224	2224	2224	2224	2224
Net Electrical Efficiency	%	42.2	41.2	40.0	41.6	40.8	40.0	43.4	42.5	41.8	43.0	42.1	41.4
CO_2 Avoidance	%	75.9	82.5	82.6	75.9	84.4	86.1	67.9	72.9	71.3	68.8	75.9	75.5
CO_2 Capture	%	84.6	88.9	89.0	84.6	90.1	91.1	78.2	81.6	80.5	78.8	83.7	83.4
Heat required in stripper reboiler	MJ/kg CO_2	1.7	1.6	1.6	1.7	1.6	1.6	1.7	1.6	1.6	1.7	1.7	1.6
H_2-rich fuel at GT inlet	TPH	95.7	80.8	78.6	95.8	81.7	75.9	95.6	82.5	81.6	99.1	83.3	80.4
Excess H_2-rich stream flow	TPH	1.4	0.5	0.7	1.5	0.8	0.3	2.0	0.7	0.1	3.0	1.4	0.8
Economic Analysis													
TCR	M$	2097	2060	2050	2070	2080	2069	1944	1937	1922	1932	1924	1918
LCOE	$/MWh	137.6	138.8	141.9	143.1	144.1	144.8	131.7	134.0	135.9	134.5	136.3	138.3
Cost of CO_2 avoidance	$/t$CO_2$	185.7	177.4	188.7	206.8	192.3	191.9	181.8	180.9	193.6	191.9	183.5	193.2

339 *Table 8: Main results from techno-economic analysis of CLR-CC process*

4.1.Behavior of the CLR

Error! Reference source not found. Figure 3, Figure 4 and Figure 5 show the main results for the performance of the CLR at different design conditions described in Table 6. **Error! Reference source not found.** Figure 3, Figure 4 and Figure 5 shows the conversion of CH_4 in the fuel reactor, the oxygen carrier flowrate in the oxidation reactor of the CLR and the syngas temperature at different air flowrates (O_2/CH_4), oxidation reactor outlet temperatures and steam/CH_4 ratios (by mass) respectively. Table 9 shows the composition of the syngas for the 12 cases defined in Table 6. The conversion of CH_4 in the fuel reactor of the CLR is a function of air flowrate (O_2/CH_4 mole ratio) in the oxidation reactor, the syngas temperature and the steam flowrate (steam/CH_4 mass ratio) in the fuel reactor. The syngas temperature anyhow is mainly dependent on the steam flowrate (steam/CH_4 mass ratio). The CH_4 conversion in the CLR is higher by 7-10% when the O_2/CH_4 mole ratio in the oxidation reactor is 0.9 when compared to 0.8. The CH_4 conversion is 3-5% higher when the steam/CH_4 mass ratio in the fuel reactor is 0.5 and decreases when the ratio is increased to 1 and 1.5. Higher steam flowrates in the fuel reactor lowers the overall fuel reactor temperature (reflected in the syngas temperature) and hence lowering the CH_4 conversion. The CH_4 conversion is 2- 4% higher when the oxidation reactor outlet temperature is changed from 1200 to 1100 °C. There is significant change in the oxygen carrier usage in the CLR when the oxidation reactor outlet temperature is changed from 1200 to 1100 °C. Lower the oxidation reactor outlet temperature, higher is the oxygen carrier circulation to maintain a steady process. The internal behavior of the oxidation and fuel reactor of the CLR in terms of the average gas and solid axial velocities, average void fractions and type of fluidization regimes is discussed further in the section.

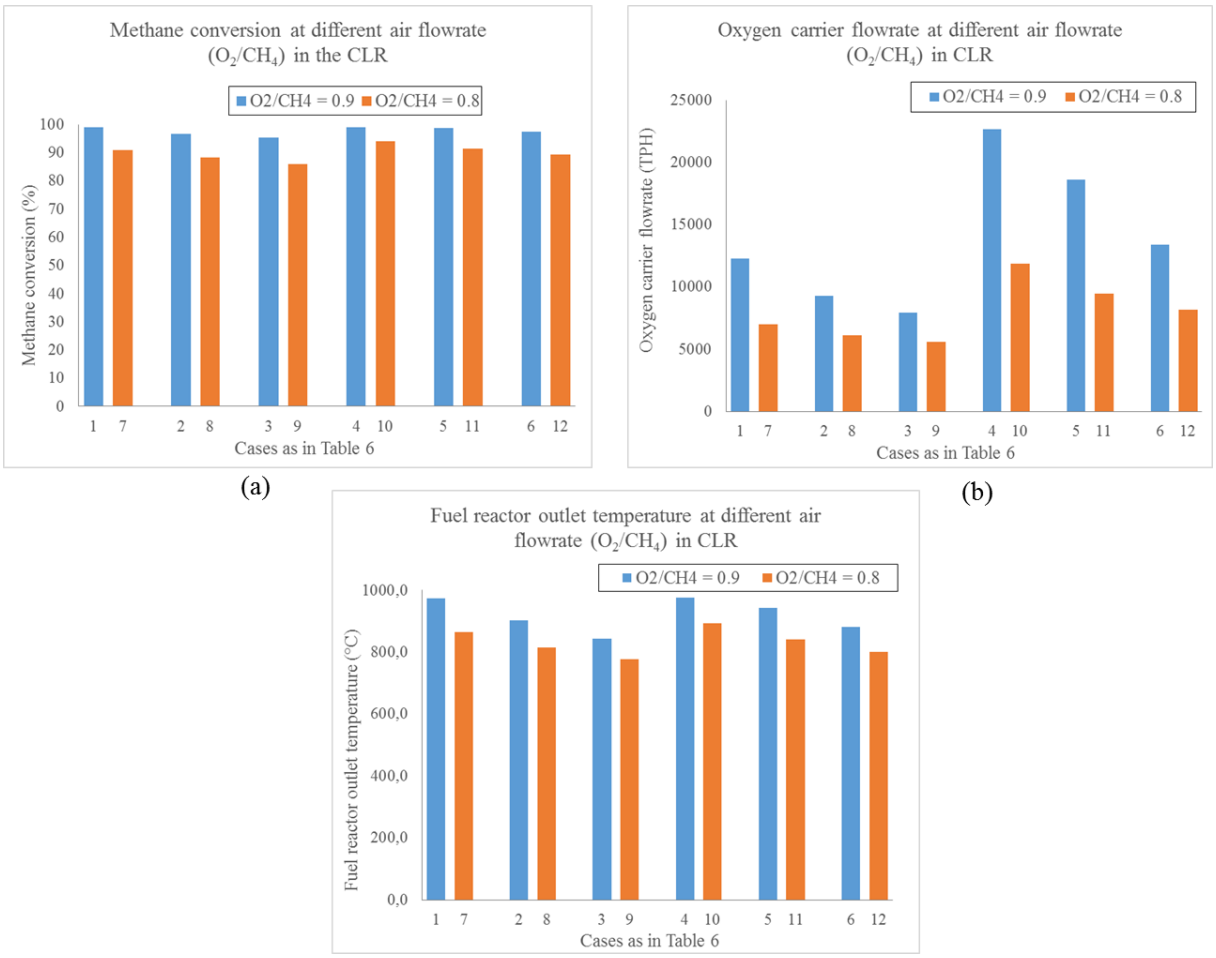

Figure 3: For different air flowrates (O_2/CH_4) (a) Methane conversion in the fuel reactor of CLR (b) Oxygen carrier flowrate in the CLR (c) Fuel reactor outlet temperature (syngas temperature)

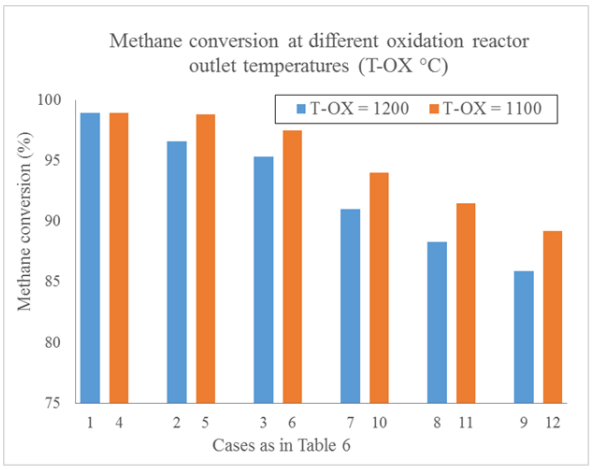

(a)

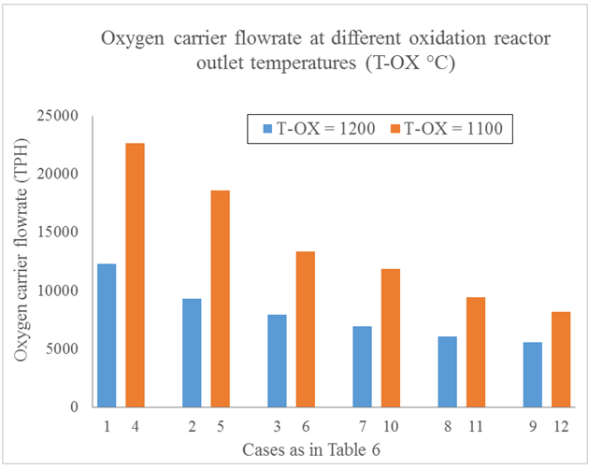

(b)

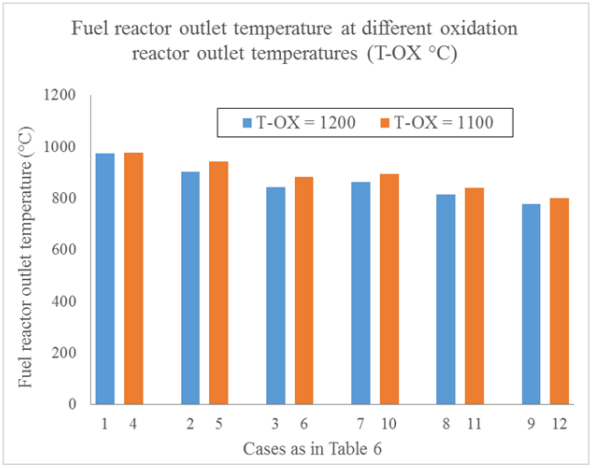

(c)

Figure 4: For different oxidation reactor outlet temperature (T-OX) (a) Methane conversion in the fuel reactor of CLR (b) Oxygen carrier flowrate in the CLR (c) Fuel reactor outlet temperature (syngas temperature)

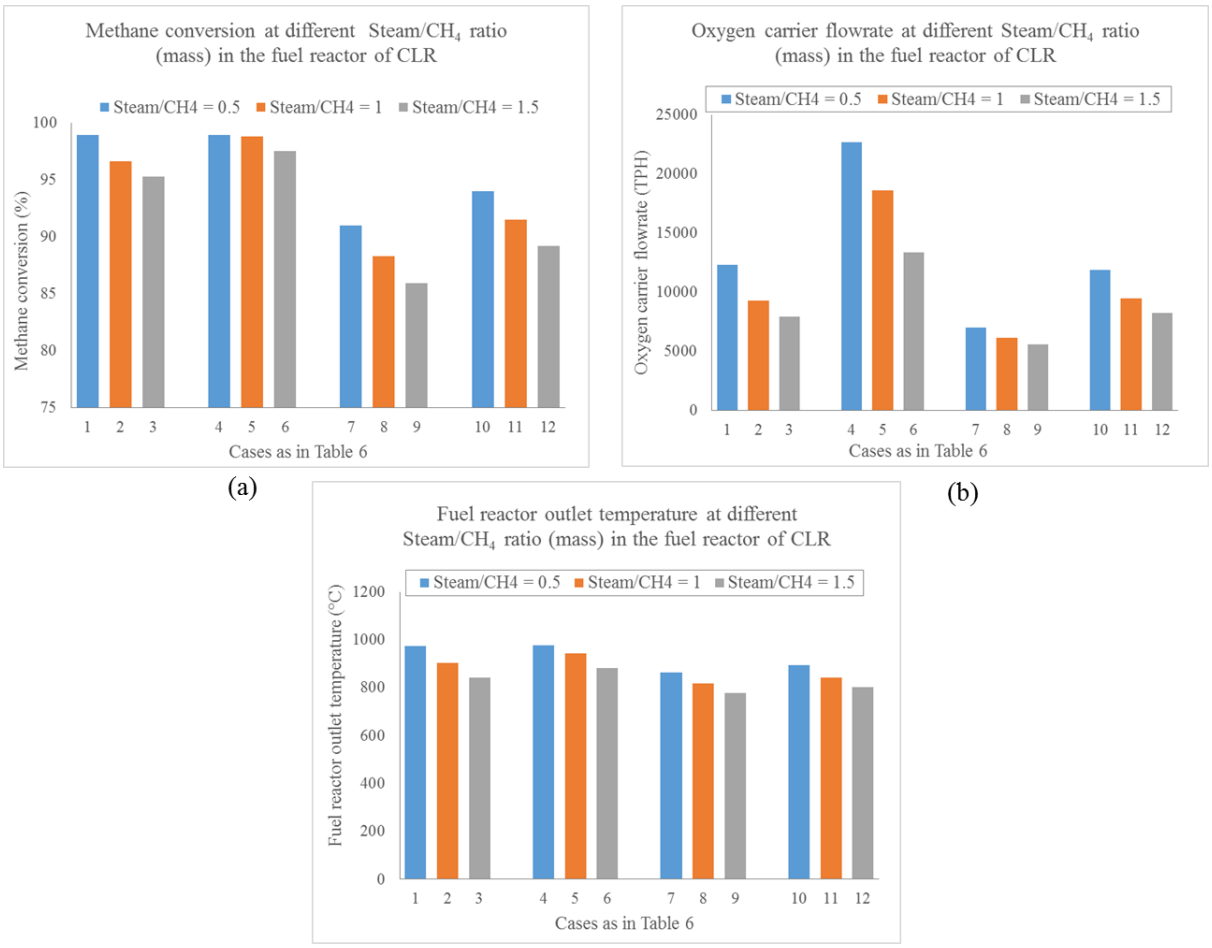

Figure 5: For different steam/CH_4 ratio (mass) in the fuel reactor of the CLR (a) Methane conversion in the fuel reactor of CLR (b) Oxygen carrier flowrate in the CLR (c) Fuel reactor outlet temperature (syngas temperature)

Cases	O_2/CH_4 by moles	Steam/CH_4 by mass	Oxidation Reactor Outlet Temperature (°C)	Syngas composition (mol%)				
				CH_4	CO	CO_2	H_2	H_2O
1	0.9	0.5	1200	0.3	20.5	8.4	42.5	28.3
2	0.9	1.0	1200	0.9	13.1	12.1	41.1	32.7
3	0.9	1.5	1200	1.1	10.8	11.7	36.6	39.8
4	0.9	0.5	1100	0.3	20.5	8.4	42.5	28.3
5	0.9	1.0	1100	0.3	15.9	9.7	39.8	34.4
6	0.9	1.5	1100	0.6	11.7	11.1	37.3	39.4
7	0.8	0.5	1200	2.7	18.7	9.2	43.8	25.5
8	0.8	1.0	1200	3.2	13.1	11.0	39.7	33.0
9	0.8	1.5	1200	3.5	9.3	11.9	36.0	39.3
10	0.8	0.5	1100	1.8	19.9	8.4	45.1	24.8
11	0.8	1.0	1100	2.3	14.3	10.3	41.1	32.1
12	0.8	1.5	1100	2.6	10.3	11.3	37.4	38.3

Table 9: Composition of syngas at the outlet of the fuel reactor of CLR

From Figure 6, it is observed that the average gas axial velocities change little with the change in the steam flowrate in the fuel reactor for the first 6 cases (O_2/CH_4 mole ratio = 0.9) which is about 1.4% in cases 1-3 and about 5% in cases 4-6. For the cases with O_2/CH_4 mole ratio as 0.8, a change in the steam/CH_4 mass ratio from 0.5 to 1.5 led to an increase in the average gas axial velocities by 9%. The average gas axial velocities are in the order of 2.62 m/s for O_2/CH_4 mole ratio of 0.9 and are lower for the cases with O_2/CH_4 mole ratio of 0.8. This decrease in the velocity with respect to the O_2/CH_4 mole ratio is due to the decrease in the methane flowrate required to maintain a steady power production at full load through the CLR-CC process. The average axial gas velocity increases by about 3% for the cases with oxidation reactor outlet temperature of 1100 °C when compared to the cases with 1200 °C.

The average solid axial velocity in the fuel reactor of the CLR for the different cases is shown in Figure 6. The solids axial velocity is affected by the change in the O_2/CH_4 mole ratio. A decrease in the O_2/CH_4 mole ratio from 0.9 to 0.8, halves the average solids axial velocity in the fuel reactor of the reactor. This behavior can be explained by the lower requirements of methane in the fuel reactor. Changes in the steam flow rate do not affect the average solids axial velocity significantly. However, for lower oxidation reactor outlet temperatures, higher axial solids velocity is observed due to higher oxygen carrier circulation.

The average void fraction in the fuel reactor of the CLR is not sensitive to the oxidation reactor outlet temperature as seen in Figure 7. However, it is affected by the steam flowrate in the fuel reactor and O_2/CH_4 mole ratio in the oxidation reactor of the CLR. An increase in steam flowrates in the fuel reactor results in an increase in the fast fluidization regime contribution and consequently higher the average void fractions in the fuel reactor. An increase of the steam/CH_4 mass ratio in the fuel reactor from 0.5 to 1.5 with O_2/CH_4 mole ratio of 0.9 leads to an increase in the void fraction by 12%. For the cases with O_2/CH_4 mole ratio of 0.8, an increase of the steam/CH_4 mass ratio in the fuel reactor from 0.5 to 1.5 increases the average void fraction by 6% in the fuel reactor.

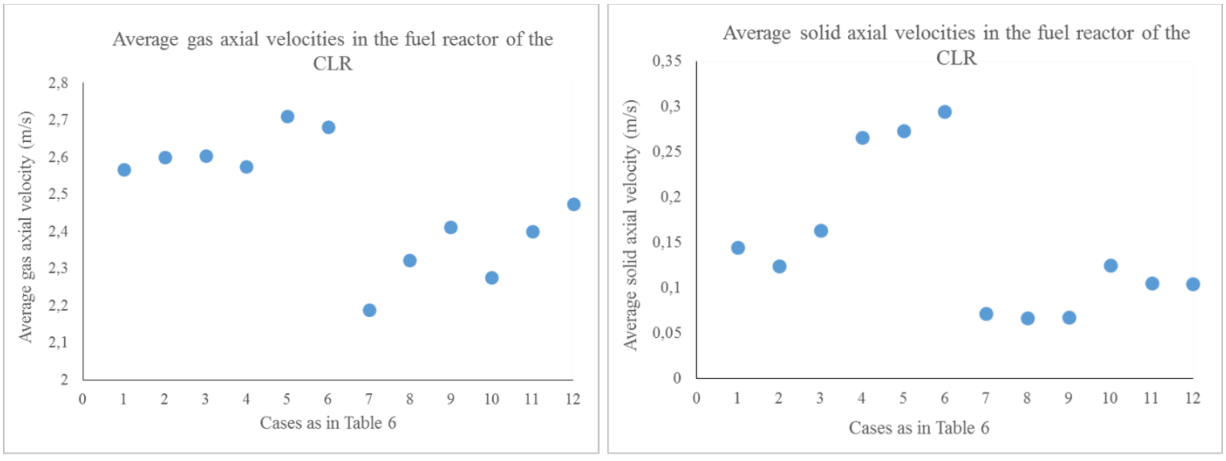

Figure 6: (a) Average gas axial velocity along the bed of the fuel reactor of the CLR (b) Average solid axial velocity along the bed of the fuel reactor of the CLR

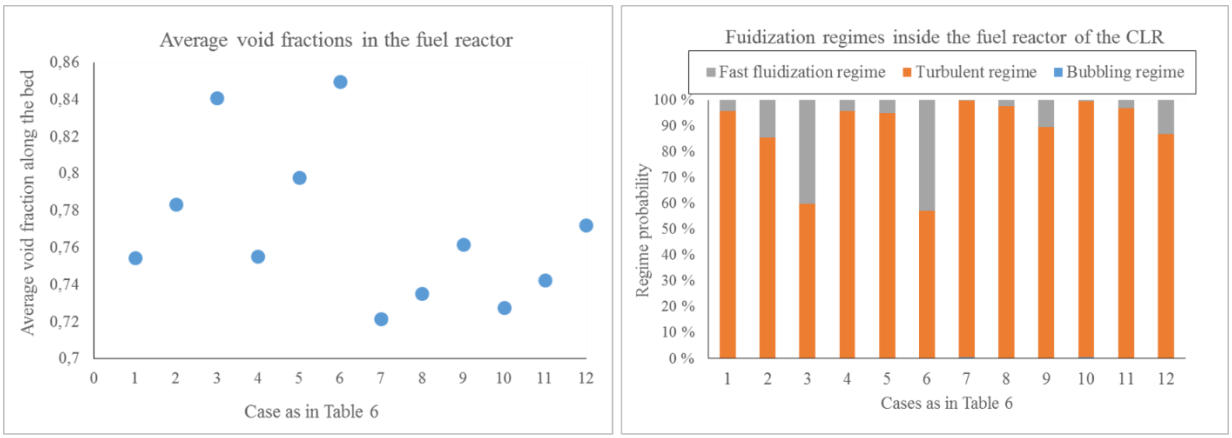

Figure 7: (a) Average void fraction in the fuel reactor of the CLR (b) Fluidization regime probabilities in the fuel reactor of the CLR

Figure 8 shows the average gas axial velocity in the oxidation reactor of the CLR. Due to lower air flowrates for cases with O_2/CH_4 mole ratio of 0.8, the average axial velocity of the gas decreases by 7-9% in the oxidation reactor when compared to cases with the O_2/CH_4 mole ratio of 0.9. Reducing the oxidation reactor outlet temperature from 1200 to 1100 °C leads to a decrease in the average gas axial velocities by 4.4% due to an increase in the gas density.

A decrease in the O_2/CH_4 mole ratio from 0.9 to 0.8 halves the average solids axial velocity in the oxidation reactor as seen in Figure 8. This is because of the lower air flowrates in the oxidation reactor when the methane requirements are low in the fuel reactor. It is also reflected in having higher contribution of the turbulent fluidization regime as seen in Figure 9. Cases 1-6 operate mostly under fast fluidization regime. Hence, the average void fraction in the oxidation reactor is 0.97 when the O_2/CH_4 mole ratio is 0.9, whereas it is 0.89 when the O_2/CH_4 mole ratio is 0.8. The higher oxygen carrier circulation at lower oxidation reactor outlet temperatures is reflected in the average solids axial velocities being higher.

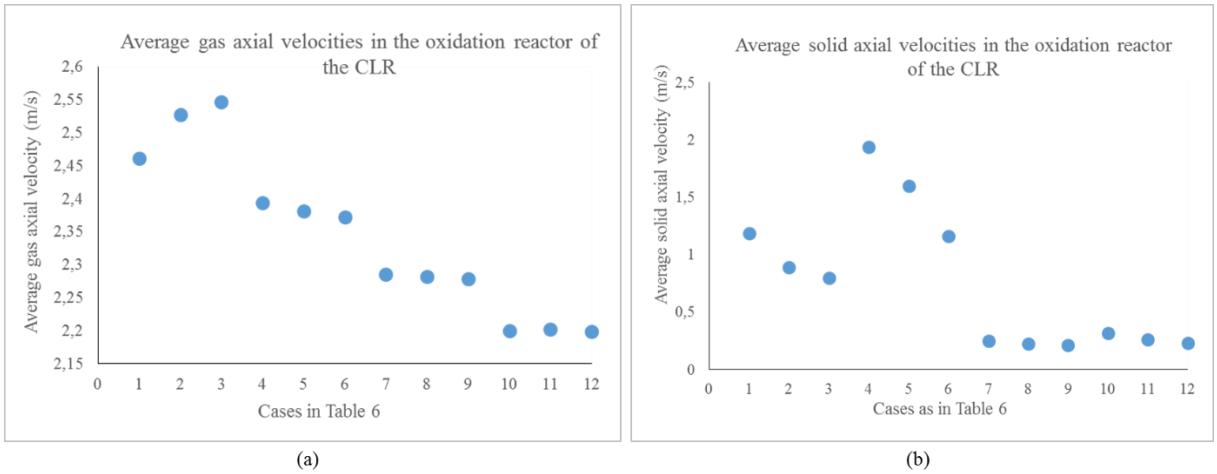

Figure 8: (a) Average gas axial velocity along the bed of the oxidation reactor of the CLR (b) Average solid axial velocity along the bed of the oxidation reactor of the CLR

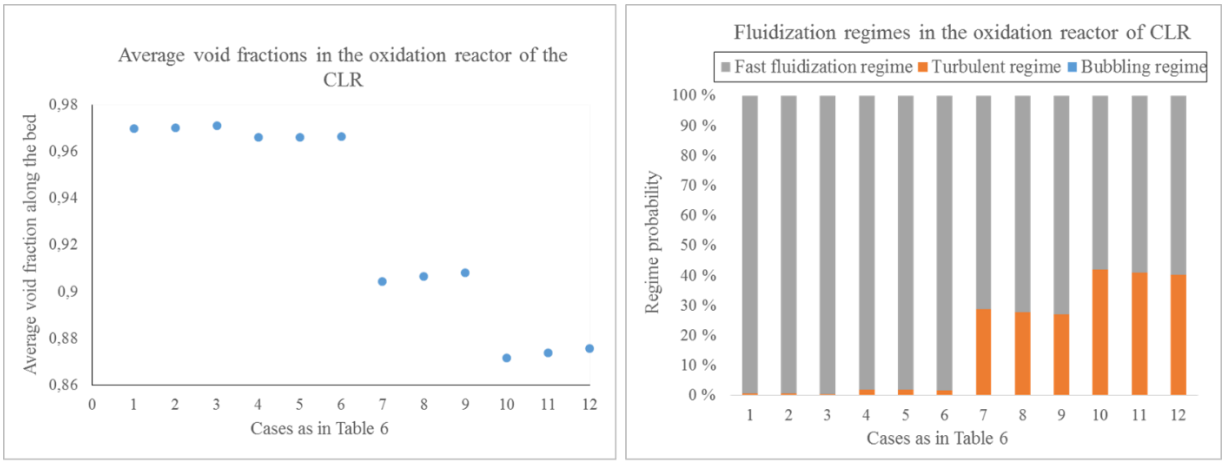

Figure 9: (a) Average void fraction in the oxidation reactor of the CLR (b) Fluidization regime probabilities in the oxidation reactor of the CLR

4.2.Technical performance analysis for the CLR-CC process

Figure 10 shows the CO_2 avoidance and net electrical efficiency for the CLR-CC process when the O_2/CH_4 mole ratio is 0.8 and 0.9 in the CLR. The O_2/CH_4 mole ratio is controlled by varying the air flowrate in the oxidation reactor of the CLR. The assumptions in the cases, for which the results are shown in Figure 10, have been defined in Table 6. The CO_2 avoidance in the CLR-CC process is higher by 8-11 % when the O_2/CH_4 is 0.9 in contrast to 0.8 in the CLR. The conversion of CH_4 in the fuel reactor is high when the O_2/CH_4 is 0.9 resulting in a higher concentration of CO_2 after the WGS step. This helps in producing a H_2-rich fuel with a higher H_2 purity and lesser concentration of CO and CH_4 (as shown in Table 10) and hence resulting in higher CO_2 avoidance for the CLR-CC process.

The net electrical efficiency for the CLR-CC process is observed to be higher by ~1.5%-points for the cases with O_2/CH_4 in the CLR as 0.8 when compared to the cases with O_2/CH_4 as 0.9 (shown in Figure 10). Four components in the CLR-CC process are mainly affected by changing the O_2/CH_4 mole ratio in the CLR. When the O_2/CH_4 mole ratio is high (=0.9), the air flowrate to the oxidation reactor is high and hence more work is consumed by the air compressor. Higher air flowrate also implicates higher N_2-rich stream flow and hence a higher power output from the N_2-rich stream turbine. The GT anyhow gives lesser power output when the O_2/CH_4 mole ratio is 0.9 when compared to 0.8. It is mainly because the H_2-rich fuel has a lower composition of CO and CH_4 when the O_2/CH_4 mole ratio is 0.9 as shown in Table 10. CO (~283 kJ/mol) and CH_4 (~802 kJ/mol) have a higher LHV than the H_2 (~244 kJ/mol). Hence, lower mole composition of CO and CH_4 in the H_2-rich fuel reflects in lower specific LHV at the inlet of the GT combustion chamber resulting in lower specific power output from the GT. Therefore, the amount of CH_4 at the inlet of fuel reactor of the CLR is high (~170 TPH) in cases with O_2/CH_4 as 0.9 when compared to 160 TPH of CH_4 in the fuel reactor of the CLR in cases with O_2/CH_4 as 0.8 for the process layout of the CLR-CC considered in this paper. Since the mass flowrate of the N_2-rich stream used as a diluent is same in all the cases, the specific power consumption in the diluent N_2-rich stream compressor is high when the O_2/CH_4 mole ratio is 0.9. The overall

efficiency penalty in the CLR-CC process is therefore high when the O_2/CH_4 mole ratio in the CLR is 0.9 and hence resulting in a lower net electrical efficiency when compared to cases that have O_2/CH_4 mole ratio of 0.8 in the CLR.

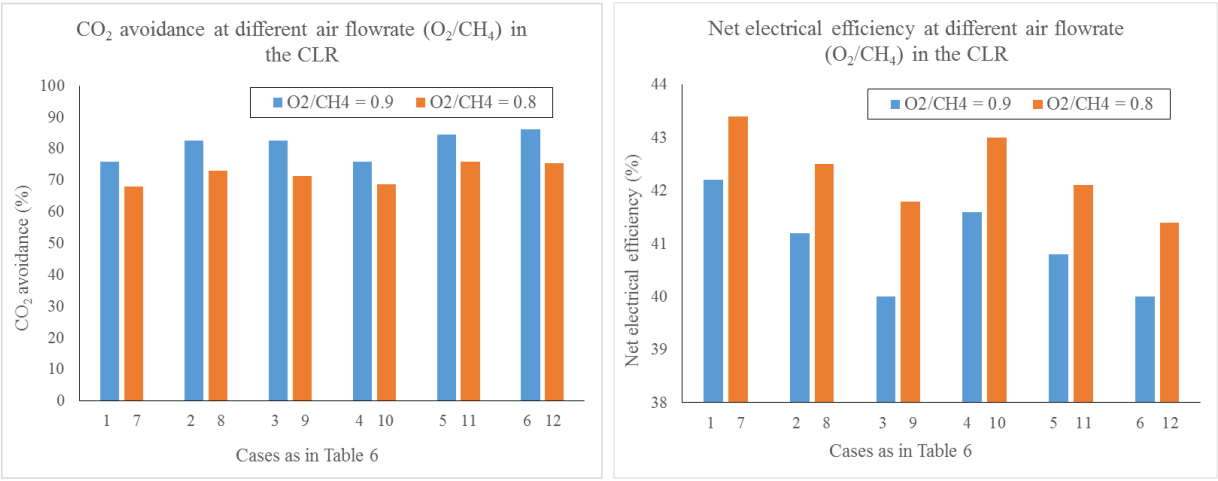

(a) (b)

Figure 10: (a) CO_2 avoidance in CLR-CC at different air flowrates (O_2/CH_4) in the CLR (b) Net electrical efficiency of CLR-CC at different air flowrates (O_2/CH_4) in the CLR

Cases	O_2/CH_4 by moles	Steam/CH_4 by mass	Oxidation Reactor Outlet Temperature (°C)	H_2-rich fuel composition (mol%)				
				H_2O	CO_2	CH_4	CO	H_2
1	0.9	0.5	1200	0.5	1.9	0.5	4.5	92.6
2	0.9	1.0	1200	0.5	2.1	1.6	1.4	94.4
3	0.9	1.5	1200	0.5	2.2	2.2	0.6	94.4
4	0.9	0.5	1100	0.5	1.9	0.5	4.5	92.6
5	0.9	1.0	1100	0.5	2.1	0.5	1.7	95.1
6	0.9	1.5	1100	0.5	2.0	1.2	0.7	95.6
7	0.8	0.5	1200	0.5	1.7	4.1	4.2	89.4
8	0.8	1.0	1200	0.5	1.8	5.6	1.2	90.8
9	0.8	1.5	1200	0.5	2.0	7.0	0.5	90.0
10	0.8	0.5	1100	0.5	1.7	2.6	5.1	90.0
11	0.8	1.0	1100	0.5	2.0	3.9	1.5	92.1
12	0.8	1.5	1100	0.5	2.0	5.1	0.6	91.7

Table 10: Composition of the H_2-rich fuel at the inlet of the combustion chamber in the gas turbine system

Figure 11 shows the CO_2 avoidance and net electrical efficiency for the CLR-CC process for different oxidation reactor outlet temperatures. The oxidation reactor outlet temperatures is controlled by the oxygen carrier flowrate in the oxidation reactor of the CLR which does not take part in the oxidation reactions and is only used to transfer heat from the oxidation reactor to the fuel reactor. In this paper, the CLR-CC process was analysed at oxidation reactor outlet temperatures of 1100 and 1200 °C. As seen in Figure 11, the CO_2 avoidance and the net electrical efficiency of the CLR-CC process is less sensitive to the oxidation reactor outlet temperatures. The CO_2 avoidance is higher by 2-4 % in the cases where the oxidation reactor outlet temperatures is assumed to be 1100 °C. More heat from the oxidation reactor is transferred to the fuel reactor of the CLR when the oxidation reactor outlet temperature is 1100

°C, which results in achieving higher conversion of CH_4 and hence a higher concentration of CO_2 at the absorber inlet of the CO_2 capture section and higher capture and avoidance rates. The net electrical efficiency of the CLR-CC is nearly 0.5% higher when the oxidation reactor outlet temperature is 1200 °C. The difference in net electrical efficiency comes from only one component, the N_2-rich stream turbine. The temperature of the N_2-rich stream from the oxidation reactor is same as the oxidation reactor outlet temperature, and hence higher the temperature, higher is the power output from the turbine.

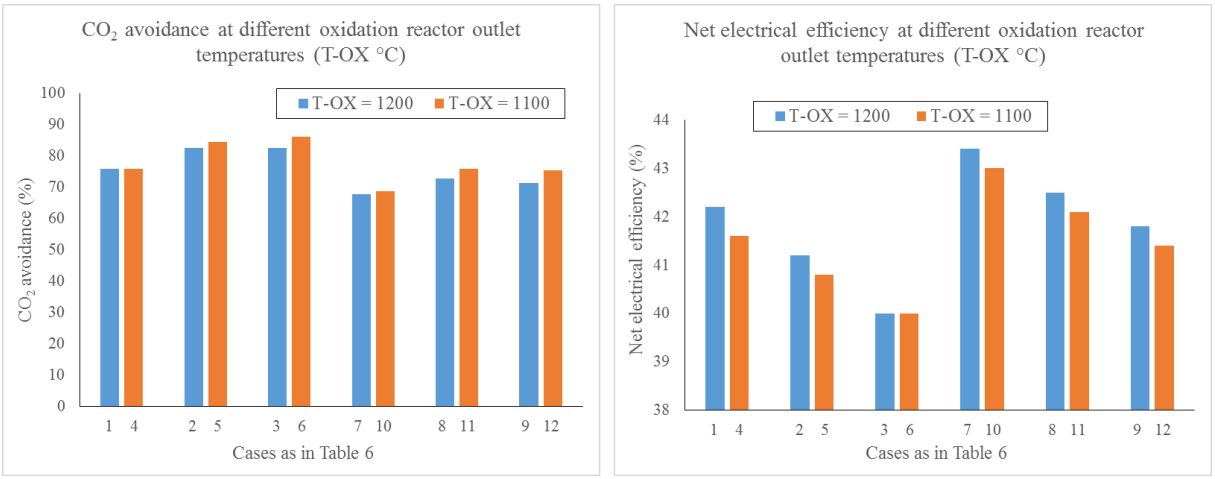

Figure 11: (a) CO_2 avoidance in CLR-CC for different oxidation reactor outlet temperatures (b) Net electrical efficiency of CLR-CC for different oxidation reactor outlet temperatures

Figure 12 shows the CO_2 avoidance and net electrical efficiency of the CLR-CC process for different steam/CH_4 ratio by mass in the fuel reactor of the CLR. The CO_2 avoidance for the CLR-CC process is 4-11 % higher when the steam/CH_4 ratio (by mass) is varied between 0.5, 1 and 1.5 in the fuel reactor of the CLR. Availability of the steam in the fuel reactor not only restricts the coke formation on the oxygen carrier in the fuel reactor, but also enhances the conversion of CO into CO_2 through a WGS reaction. Hence, the concentration of CO_2 is high in the syngas (as seen in Table 9) and the stream at the absorber inlet of the CO_2 capture section, when the steam/CH_4 ratio in the fuel reactor is high, resulting in a higher CO_2 avoidance rate for the CLR-CC. The net electrical efficiency of the CLR-CC decreases by ~1% for every 0.5 point increase in the steam/CH_4 mass ratio in the fuel reactor. The ST in the power plant directly affects the net electrical efficiency. Steam for the fuel reactor is extracted from the MP steam turbine. Therefore, at higher steam/CH_4 mass ratio in the fuel reactor, more amount of steam is extracted from the ST resulting in lower power output from the ST system.

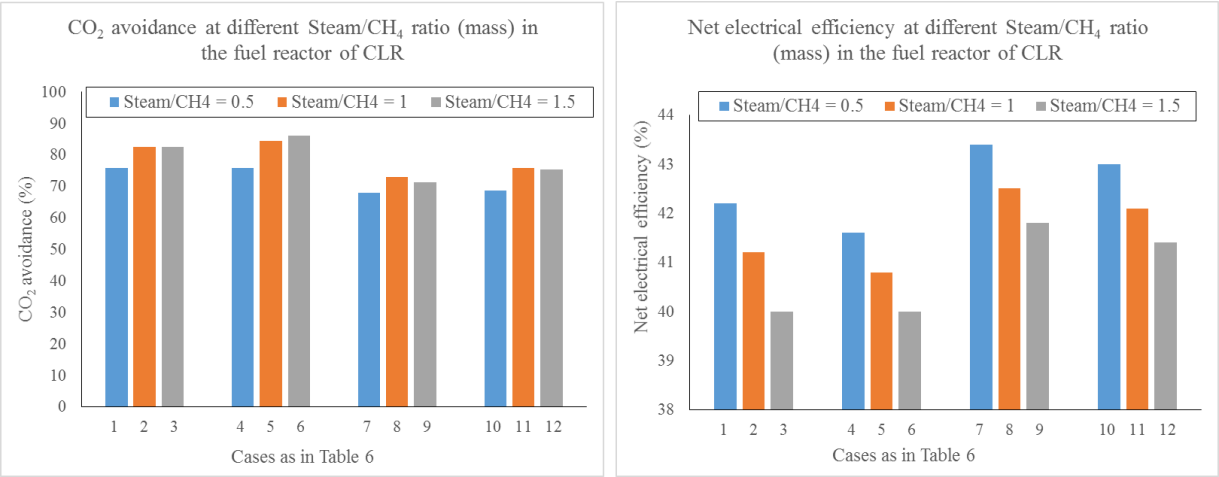

(a) (b)

Figure 12: (a) CO_2 avoidance in CLR-CC at different steam/CH_4 mass ratio in the fuel reactor of CLR (b) Net electrical efficiency of CLR-CC at different steam/CH_4 mass ratio in the fuel reactor of CLR

4.3.Economic analysis of the CLR-CC process

The main results from the economic analysis for the CLR-CC are shown in Table 8 for different cases studied in this paper. Figure 13 shows the contribution of TCR, FOM, VOM and FC to the LCOE of the CLR-CC whereas Figure 14 shows the contribution of capital costs of different sections in the process to the BEC. The LCOE for the CLR-CC process is 4-7 $/MWh less when the O_2/CH_4 mole ratio in the CLR is 0.8 when compared to the cases having O_2/CH_4 mole ratio of 0.9 in the CLR. The main difference is observed in the TCR and the FC. For O_2/CH_4 mole ratio of 0.9 in the CLR, the flowrate and temperature of syngas is high. Hence, the amount of steam produced in cooling of syngas and the product streams from HTS and LTS is high, which demands more heat exchange area. Therefore, as seen in Figure 14**Error! Reference source not found.**, the BEC of the components associated with N_2-rich stream treatment is higher. Although less significant, but the VOM is slightly more when the O_2/CH_4 mole ratio is 0.9 in the CLR. This is mainly due to the costs incurred by higher requirement of oxygen carrier. The CLR-CC process also requires higher CH_4 input to the fuel reactor for the cases with O_2/CH_4 mole ratio of 0.9, and hence the FC is high when the O_2/CH_4 mole ratio is 0.9.

The LCOE of the CLR-CC is 3-6 $/MWh less for the cases with oxidation reactor outlet temperature of 1200 °C when compared to the cases for which the temperature is 1100 °C. The difference in LCOE is due to the higher VOM in the cases with oxidation reactor outlet temperature of 1100 °C because of the higher oxygen carrier utilization in the CLR. There is no significant difference in the other components of the LCOE at different oxidation reactor outlet temperatures.

The steam/CH_4 mass ratio in the CLR has less effect on the LCOE of the CLR-CC process. The LCOE of the CLR-CC changes by ~1 $/MWh for a change of 0.5 in the steam/CH_4 mass ratio in the fuel reactor of the CLR. The LCOE is less for the cases with higher net electrical efficiency because the fuel consumption for 1MWh electricity produced is less, and hence the FC component of the LCOE is lower.

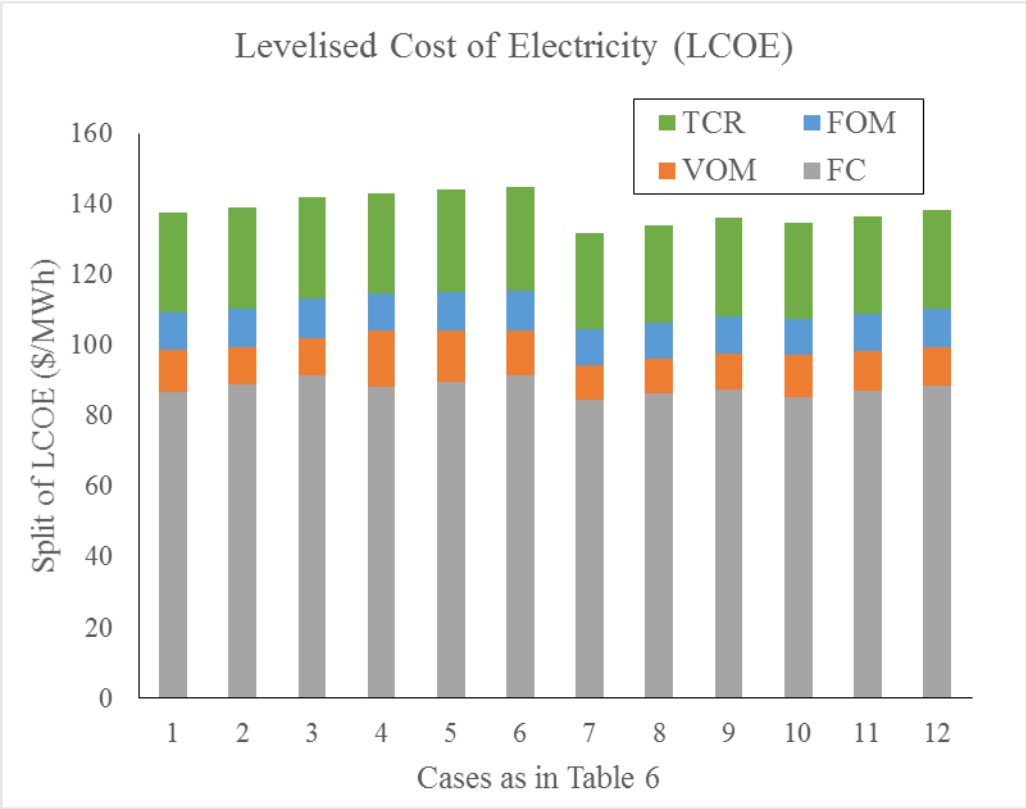

533

534 *Figure 13: Contribution of the TCR, FOM, VOM and FC to the LCOE of the CLR-CC process for different cases*
535 *defined in Table 6*

536

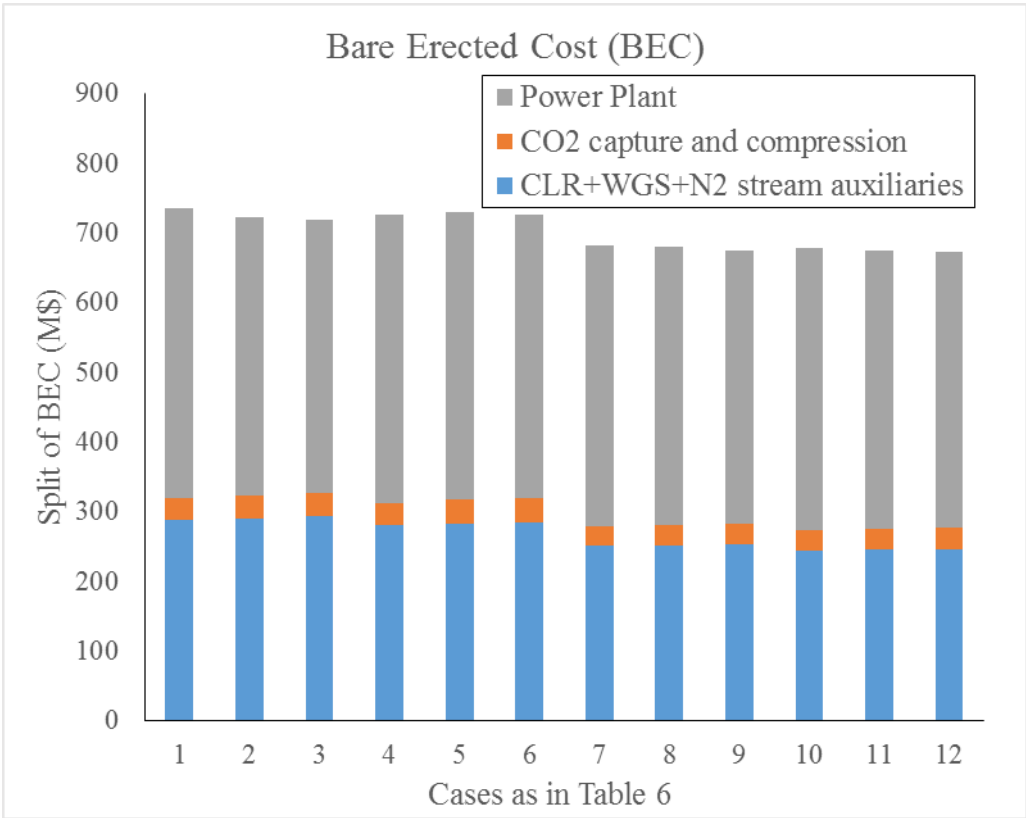

537

538 *Figure 14: Bare erected cost for the CLR-CC for different cases defined in Table 6*

4.4. Effect of fuel cost and process contingency on LCOE

Error! Reference source not found. Figure 13 clearly shows that the major contributors to the LCOE of the process is the fuel costs and the TCR. While estimating the TCR of the CLR-CC process, the process contingency was assumed 50% of BEC, which is for a process which is considered to be a new concept with limited data (GCCSI 2013). The fuel cost was assumed 10.18 $/GJ-LHV. Anyhow, the process contingency of the process depends completely on its level of maturity whereas the fuel cost is very much dependent on the region from where it is imported. **Error! Reference source not found.** Figure 15 provides a sensitivity study for the defined cases when the process contingency is 50% and 10% of BEC, and the fuel cost is 10.18 and 4.5 $/GJ-LHV. As seen in Figure 15**Error! Reference source not found.**, the LCOE for the CLR-CC process varies between 75.3 and 144.8 $/MWh.

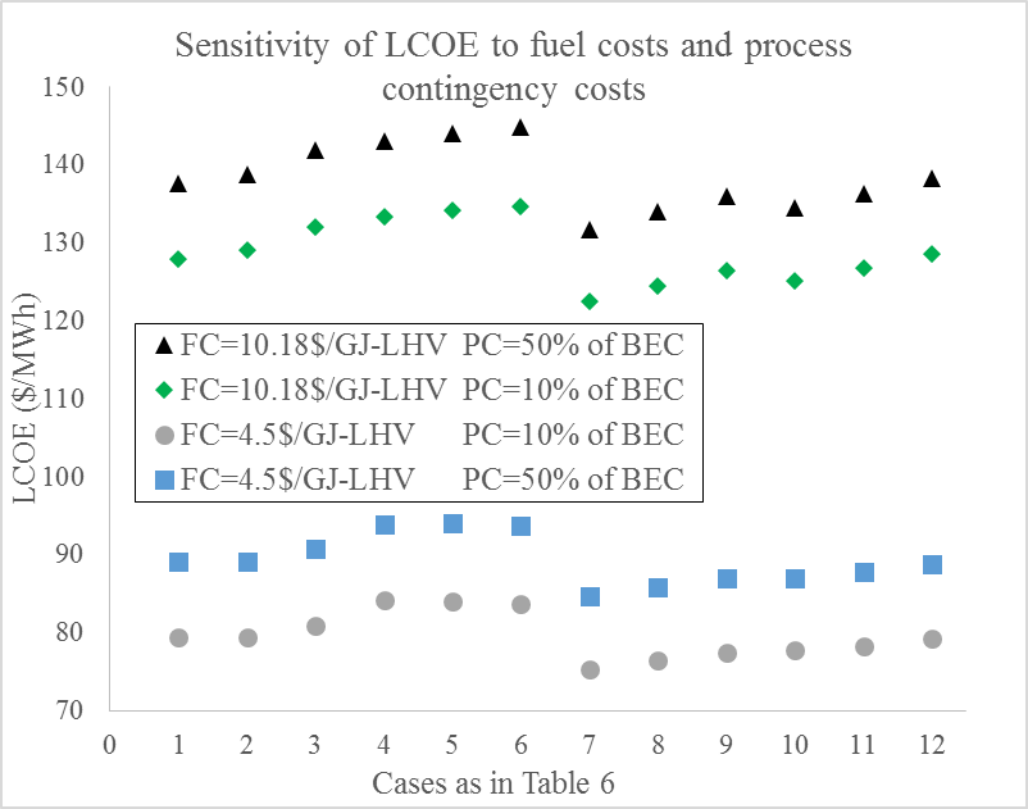

Figure 15: Sensitivity of LCOE to fuel cost and process contingency

5. Conclusion

This paper presents the techno-economic analysis of the CLR-CC process. The conditions in the CLR were simulated using the 1-D phenomenological model developed by Francisco Morgado et al. (2016). The process layout for the CLR-CC was discussed and a sensitivity study with respect to the pressure inside the CLR was presented by Nazir, Bolland, and Amini (2018). In this paper, three manipulative variables, air flowrate (O_2/CH_4 molar ratio) at the inlet of oxidation reactor, oxidation reactor outlet temperature and steam flow rate (steam/CH_4 mass

ratio) to the fuel reactor, were selected. The effect of changes in these variables on the overall techno-economic performance of the CLR-CC process was analysed over 12 different cases. The main techno-economic performance indicators of the process are CH_4 conversion in the fuel reactor, CO_2 avoidance rates, net electrical efficiency and the LCOE. The CH_4 conversion in the fuel reactor is between 85-99% and is highly sensitive to the air flowrate (O_2/CH_4 mole ratio) in the CLR. The CO_2 avoidance rates in the CLR-CC is between 67-86%. The CO_2 avoidance is highly sensitive to the air flowrate (O_2/CH_4 mole ratio) in the oxidation reactor followed by the steam flow rate (steam/CH_4 mass ratio) in the fuel reactor of the CLR. The net electrical efficiency of the CLR-CC is between 40-43.5% for the cases studied in this paper. The net electrical efficiency is sensitive to the O_2/CH_4 mole ratio in the CLR and the steam/CH_4 mass ratio in the fuel reactor of the CLR. The net electrical efficiency is higher when the O_2/CH_4 mole ratio in the CLR is 0.8 when compared to 0.9, and the net electrical efficiency decreases with an increase in steam/CH_4 mass ratio in the fuel reactor. The LCOE for the CLR-CC lies between 131-145 $/MWh. The LCOE of the CLR-CC is less sensitive to the process parameters and is highly sensitive to the NG price (fuel costs) followed by the process contingencies cost. The LCOE is reduced by 40% if the NG price is halved whereas if the process contingency is reduced from 50% (for a new technology) to 10% (more mature and commercially available technology), the LCOE reduces by ~10%.

The CO_2 avoidance in the CLR-CC is on par with other pre- and post-combustion capture methods. Anyhow, the net electrical efficiency of the CLR-CC for the conditions reported in this paper is close to the net electrical efficiency of a combined cycle with steam-methane reforming (~43.6%) but is less than that of combined cycles with auto-thermal reforming (~46.9) and post-combustion capture methods involving chemical absorption (~49-50%). The efficiency of the CLR-CC process is also limited by the gas turbine design. One of the major benefits from the CLR-CC process when compared to the post-combustion capture methods is the flexibility in operating the plant based on the needed output which could be H_2 or electric power. The current analysis helps in understanding the trends and techno-economic behavior of the CLR-CC process for the chosen manipulated variables. Improving efficiency of the process will help in reducing fuel consumption and hence reducing the costs. Therefore, further optimization studies for the CLR-CC process is suggested. The developed methods in this paper can also be applied to analyzing novel reactor concepts for reforming like the gas-switching reforming (Wassie et al. 2017).

6. Acknowledgements

This publication forms a part of the EU-FP7 project titled “A Multiscale Simulation-Based Design Platform for Cost-Effective CO_2 Capture Processes using Nano-Structured Materials (NanoSim)” and project number 604656. The authors thank the European Commission for the funding. The authors would also like to acknowledge the partners: SINTEF Industry, Universidade de Coimbra, ANDRITZ Energy & Environment GmbH, DCS Computing GmbH, Institut National Polytechnique de Toulouse (INPT), University College London, Technische Universitaet Graz for their support.

References

Abanades, J. C., R. Murillo, J. R. Fernandez, G. Grasa, and I. Martínez. 2010. "New CO2 capture process for hydrogen production combining Ca and Cu chemical loops." *Environmental Science and Technology* 44 (17):6901-6904. doi: 10.1021/es101707t.

Abba, I. a, J. R. Grace, H. T. Bi, and M. L. Thompson. 2003. "Spanning the flow regimes: Generic fluidized-bed reactor model." *AIChE Journal* 49:1838-1848. doi: 10.1002/aic.690490720.

Adanez, J., A. Abad, F. Garcia-Labiano, P. Gayan, and L. F. De Diego. 2012. "Progress in chemical-looping combustion and reforming technologies." *Progress in Energy and Combustion Science* 38 (2):215-282. doi: 10.1016/j.pecs.2011.09.001.

Antzara, A., E. Heracleous, D. B. Bukur, and A. A. Lemonidou. 2015. "Thermodynamic analysis of hydrogen production via chemical looping steam methane reforming coupled with in situ CO2 capture." *International Journal of Greenhouse Gas Control* 32 (0):115-128. doi: http://dx.doi.org/10.1016/j.ijggc.2014.11.010.

AspenHYSYS. 2017. Aspen HYSYS V8.6 User Guide. Aspen Technology Inc., Bedford, Massachusetts, USA.

Bischi, A., Ø Langørgen, J. X. Morin, J. Bakken, M. Ghorbaniyan, M. Bysveen, and O. Bolland. 2012. "Hydrodynamic viability of chemical looping processes by means of cold flow model investigation." *Applied Energy* 97:201-216. doi: 10.1016/j.apenergy.2011.12.051.

Boot-Handford, M. E., J. C. Abanades, E. J. Anthony, M. J. Blunt, S. Brandani, N. Mac Dowell, J. R. Fernández, M. C. Ferrari, R. Gross, J. P. Hallett, R. S. Haszeldine, P. Heptonstall, A. Lyngfelt, Z. Makuch, E. Mangano, R. T. J. Porter, M. Pourkashanian, G. T. Rochelle, N. Shah, J. G. Yao, and P. S. Fennell. 2014. "Carbon capture and storage update." *Energy and Environmental Science* 7 (1):130-189.

Chiesa, Paolo, Giovanni Lozza, and Luigi Mazzocchi. 2005. "Using Hydrogen as Gas Turbine Fuel." *Journal of Engineering for Gas Turbines and Power* 127 (1):73-80. doi: 10.1115/1.1787513.

Consonni, S., G. Lozza, G. Pelliccia, S. Rossini, and F. Saviano. 2006. "Chemical-looping combustion for combined cycles with CO2 capture." *Journal of Engineering for Gas Turbines and Power* 128 (3):525-534. doi: 10.1115/1.1850501.

Cormos, C. C. 2012. "Evaluation of syngas-based chemical looping applications for hydrogen and power co-generation with CCS." *International Journal of Hydrogen Energy* 37 (18):13371-13386. doi: 10.1016/j.ijhydene.2012.06.090.

Cormos, C. C., L. Petrescu, and A. M. Cormos. 2014. Assessment of hydrogen production systems based on natural gas conversion with carbon capture and storage. In *Computer Aided Chemical Engineering*.

Corradetti, Alessandro, and Umberto Desideri. 2005. "Analysis of Gas-Steam Combined Cycles With Natural Gas Reforming and CO2 Capture." *Journal of Engineering for Gas Turbines and Power* 127 (3):545-552. doi: 10.1115/1.1850941.

de Diego, L. F., M. Ortiz, F. García-Labiano, J. Adánez, A. Abad, and P. Gayán. 2009. "Hydrogen production by chemical-looping reforming in a circulating fluidized bed reactor using Ni-based oxygen carriers." *Journal of Power Sources* 192 (1):27-34. doi: 10.1016/j.jpowsour.2008.11.038.

Diglio, Giuseppe, Piero Bareschino, Erasmo Mancusi, and Francesco Pepe. 2016. "Simulation of hydrogen production through chemical looping reforming process in a packed-bed reactor." *Chemical Engineering Research and Design* 105:137-151. doi: http://dx.doi.org/10.1016/j.cherd.2015.11.013.

Ding, O. L., and S. H. Chan. 2008. "Autothermal reforming of methane gas—Modelling and experimental validation." *International Journal of Hydrogen Energy* 33 (2):633-643. doi: http://dx.doi.org/10.1016/j.ijhydene.2007.10.037.

DOE/NETL. 2007. Cost and Performance Baseline for Fossil Energy Plants.

EBTF. 2011. European best practice guidelines for assessment of CO2 capture technologies. CESAR -project 7th FrameWork Programme. Collaborative Project– GA No. 213569.

ETP. 2012. Energy Technology Perspectives 2012. International Energy Agency.

Fan, J., and L. Zhu. 2015. "Performance analysis of a feasible technology for power and high-purity hydrogen production driven by methane fuel." *Applied Thermal Engineering* 75:103-114. doi: 10.1016/j.applthermaleng.2014.10.013.

Fiaschi, Daniele, Francesco Gamberi, Michael Bartlett, and Timothy Griffin. 2005. "The air membrane-ATR integrated gas turbine power cycle: A method for producing electricity with low CO2 emissions." *Energy Conversion and Management* 46 (15–16):2514-2529. doi: http://dx.doi.org/10.1016/j.enconman.2004.11.008.

Francisco Morgado, J., S. Cloete, J. Morud, T. Gurker, and S. Amini. 2016. "Modelling study of two chemical looping reforming reactor configurations: Looping vs. switching." *Powder Technology*. doi: 10.1016/j.powtec.2016.11.059.

GCCSI. 2013. Global CCS Institute - TOWARD A COMMON METHOD OF COST ESTIMATION FOR CO2 CAPTURE AND STORAGE AT FOSSIL FUEL POWER PLANTS.

Iloeje, C., Z. Zhao, and A. F. Ghoniem. 2015. "Analysis of thermally coupled chemical looping combustion-based power plants with carbon capture." *International Journal of Greenhouse Gas Control* 35:56-70. doi: 10.1016/j.ijggc.2015.01.013.

Ishida, M., D. Zheng, and T. Akehata. 1987. "Evaluation of a chemical-looping-combustion power-generation system by graphic exergy analysis." *Energy* 12 (2):147-154. doi: http://dx.doi.org/10.1016/0360-5442(87)90119-8.

Ishida, Masaru, and Hongguang Jin. 1994. "A new advanced power-generation system using chemical-looping combustion." *Energy* 19 (4):415-422. doi: http://dx.doi.org/10.1016/0360-5442(94)90120-1.

Kolbitsch, P., T. Pröll, J. Bolhar-Nordenkampf, and H. Hofbauer. 2009. "Design of a Chemical Looping Combustor using a Dual Circulating Fluidized Bed (DCFB) Reactor System." *Chemical Engineering & Technology* 32 (3):398-403. doi: 10.1002/ceat.200800378.

Kvamsdal, H. M., K. Jordal, and O. Bolland. 2007. "A quantitative comparison of gas turbine cycles with CO2 capture." *Energy* 32 (1):10-24. doi: 10.1016/j.energy.2006.02.006.

Lozza, G., and P. Chiesa. 2000a. "Natural Gas Decarbonization to Reduce CO2 Emission From Combined Cycles—Part I: Partial Oxidation." *Journal of Engineering for Gas Turbines and Power* 124 (1):82-88. doi: 10.1115/1.1395581.

Lozza, G., and P. Chiesa. 2000b. "Natural Gas Decarbonization to Reduce CO2 Emission From Combined Cycles—Part II: Steam-Methane Reforming." *Journal of Engineering for Gas Turbines and Power* 124 (1):89-95. doi: 10.1115/1.1395582.

Mantripragada, H. C., and E. S. Rubin. 2013. "Chemical looping for pre-combustion CO2 capture - Performance and cost analysis." Energy Procedia.

Martínez, I., R. Murillo, G. Grasa, J. R. Fernández, and J. C. Abanades. 2013. "Integrated combined cycle from natural gas with CO2 capture using a Ca-Cu chemical loop." *AIChE Journal* 59 (8):2780-2794. doi: 10.1002/aic.14054.

Martínez, I., M. C. Romano, J. R. Fernández, P. Chiesa, R. Murillo, and J. C. Abanades. 2014. "Process design of a hydrogen production plant from natural gas with CO2 capture based on a novel Ca/Cu chemical loop." *Applied Energy* 114 (0):192-208. doi: http://dx.doi.org/10.1016/j.apenergy.2013.09.026.

Mathieu, Philippe, and Olav Bolland. 2013. "Comparison of Costs for Natural gas Power Generation with CO2 Capture." *Energy Procedia* 37 (0):2406-2419. doi: http://dx.doi.org/10.1016/j.egypro.2013.06.122.

Morgado, Joana Francisco, Schalk Cloete, John Morud, Thomas Gurker, and Shahriar Amini. 2016. "Modelling study of two chemical looping reforming reactor configurations: Looping vs. switching." *Powder Technology* In Press. doi: http://dx.doi.org/10.1016/j.powtec.2016.11.059.

Naqvi, R., and O. Bolland. 2007. "Multi-stage chemical looping combustion (CLC) for combined cycles with CO2 capture." *International Journal of Greenhouse Gas Control* 1 (1):19-30. doi: 10.1016/S1750-5836(07)00012-6.

Nazir, Shareq, Olav Bolland, and Shahriar Amini. 2018. "Analysis of Combined Cycle Power Plants with Chemical Looping Reforming of Natural Gas and Pre-Combustion CO2 Capture." *Energies* 11 (1):147.

Nazir, Shareq Mohd, Olav Bolland, and Shahriar Amini. 2017. "Full Plant Scale Analysis of Natural Gas Fired Power Plants with Pre-Combustion CO2 Capture and Chemical Looping Reforming (CLR)." *Energy Procedia* 114:2146-2155. doi: http://dx.doi.org/10.1016/j.egypro.2017.03.1350.

NETL. 2011. Cost Estimation Methodology for NETL Assessments of Power Plant Performance.

Nord, Lars Olof, Rahul Anantharaman, and Olav Bolland. 2009. "Design and off-design analyses of a pre-combustion CO2 capture process in a natural gas combined cycle power plant." *International Journal of Greenhouse Gas Control* 3 (4):385-392. doi: http://dx.doi.org/10.1016/j.ijggc.2009.02.001.

Peters, Max S., and Klaus D. Timmerhaus. 1991. *PLANT DESIGN AND ECONOMICS FOR CHEMICAL ENGINEERS*. Fourth Edition ed: McGraw-Hill, Inc.

Pröll, T., J. Bolhàr-Nordenkampf, P. Kolbitsch, and H. Hofbauer. 2010. "Syngas and a separate nitrogen/argon stream via chemical looping reforming - A 140 kW pilot plant study." *Fuel* 89 (6):1249-1256. doi: 10.1016/j.fuel.2009.09.033.

Pröll, T., P. Kolbitsch, J. Bolhàr-Nordenkampf, and H. Hofbauer. 2011. "Chemical looping pilot plant results using a nickel-based oxygen carrier." *Oil and Gas Science and Technology* 66 (2):173-180. doi: 10.2516/ogst/2010036.

Pröll, Tobias, Hermann Hofbauer, Philipp Kolbitsch, and Johannes Bolhàr-Nordenkampf. The Dual Circulating Fluidized Bed (DCFB) Reactor System edited by Technology Transfer at Vienna University of Technology.

Richter, Horst J., and Karl F. Knoche. 1983. "REVERSIBILITY OF COMBUSTION PROCESSES." *ACS Symposium Series*:71-85.

Romano, Matteo C., Paolo Chiesa, and Giovanni Lozza. 2010. "Pre-combustion CO2 capture from natural gas power plants, with ATR and MDEA processes." *International Journal of Greenhouse Gas Control* 4 (5):785-797. doi: http://dx.doi.org/10.1016/j.ijggc.2010.04.015.

Rydén, M., A. Lyngfelt, and T. Mattisson. 2006. "Synthesis gas generation by chemical-looping reforming in a continuously operating laboratory reactor." *Fuel* 85 (12-13):1631-1641. doi: 10.1016/j.fuel.2006.02.004.

Schmid, J. C., C. Pfeifer, H. Kitzler, Tobias Proll, and Hermann Hofbauer. 2011. "A new dual fluidized bed gasifier design for improved in situ conversion of hydrocarbons." *Proceedings International Conference on Polygeneration Strategies (ICPS)*.

Spallina, V., D. Pandolfo, A. Battistella, M. C. Romano, M. Van Sint Annaland, and F. Gallucci. 2016. "Techno-economic assessment of membrane assisted fluidized bed reactors for pure H2 production with CO2 capture." *Energy Conversion and Management* 120:257-273. doi: http://dx.doi.org/10.1016/j.enconman.2016.04.073.

Spallina, Vincenzo, Fausto Gallucci, Matteo C. Romano, and Martin Van Sint Annaland. 2016. "Pre-combustion packed bed chemical looping (PCCL) technology for efficient H2-rich gas production processes." *Chemical Engineering Journal* 294:478-494. doi: http://dx.doi.org/10.1016/j.cej.2016.03.011.

Tang, M., L. Xu, and M. Fan. 2015. "Progress in oxygen carrier development of methane-based chemical-looping reforming: A review." *Applied Energy* 151. doi: 10.1016/j.apenergy.2015.04.017.

Thermoflow. 2017. Thermoflow Suite V26 User Guide. Thermoflow Inc., Southborough, MA, USA.

Thompson, Michael L., Hsiaotao Bi, and John R. Grace. 1999. "A generalized bubbling / turbulent fuidized-bed reactor model." *Chemical Engineering Science* 54:3-10.

Wassie, Solomon A., Fausto Gallucci, Abdelghafour Zaabout, Schalk Cloete, Shahriar Amini, and Martin van Sint Annaland. 2017. "Hydrogen production with integrated CO2 capture in a novel gas switching reforming reactor: Proof-of-concept." *International Journal of Hydrogen Energy* 42 (21):14367-14379. doi: https://doi.org/10.1016/j.ijhydene.2017.04.227.

WEO. 2016. World Energy Outlook 2016. International Energy Agency.

Yahom, A., J. Powell, V. Pavarajarn, P. Onbhuddha, S. Charojrochkul, and S. Assabumrungrat. 2014. "Simulation and thermodynamic analysis of chemical looping reforming and CO2 enhanced chemical looping reforming." *Chemical Engineering Research and Design* 92 (11):2575-2583. doi: 10.1016/j.cherd.2014.04.002.

Zohrabian, Angineh, Mohammad Mansouri Majoumerd, Mohammad Soltanieh, and Sourena Sattari. 2016. "Techno-economic evaluation of an integrated hydrogen and power co-generation system with CO2 capture." *International Journal of Greenhouse Gas Control* 44:94-103. doi: http://dx.doi.org/10.1016/j.ijggc.2015.11.004.